RSC Advances

PAPER

View Article Online
View Journal | View Issue

Cite this: *RSC Adv.*, 2014, **4**, 2764

A novel molecularly imprinted polymer on CdSe/ZnS quantum dots for highly selective optosensing of mycotoxin zearalenone in cereal samples†

Guozhen Fang, Chao Fan, Huilin Liu, Mingfei Pan, Huidan Zhu and Shuo Wang*

Received 17th September 2013
Accepted 26th November 2013

DOI: 10.1039/c3ra45172k

www.rsc.org/advances

A novel molecularly imprinted optosensing material (MIOM) based on ionic liquid (IL)-stabilized CdSe/ZnS quantum dots (QDs) was prepared, for highly selective and sensitive recognition of the mycotoxin zearalenone (ZON). ZON is expensive and highly toxic, so the ZON analog cyclodo-decanyl-2,4-dihydroxybenzoate (CDHB) was instead used as the template. MIOM was characterized by scanning electron microscopy (SEM), Fourier transform infrared spectroscopy (FT-IR) and adsorption experiment. Under optimal conditions, the relative fluorescence intensity of MIOM decreased linearly with increasing ZON concentration, in the range of 0.003–3.12 μmol L^{-1}. MIOM had a detection limit of 0.002 μmol L^{-1}. MIOM was used to detect ZON in corn, rice and wheat flours, and at three concentration levels 50, 100 and 500 ng g^{-1}, ZON recoveries for these three cereals were 94.2–98.7%, 93.1–107.6% and 84.4–106.0%, respectively.

Introduction

Molecular imprinting is used to synthesize polymers with special binding sites closely matching the template. Wulff and Sarchan prepared the first molecularly imprinted polymer (MIP).[1] Mosbach *et al.* reported molecular imprints of theophylline and diazepam in 1993, which greatly promoted the development of MIPs.[2] MIPs have advantages to biological antibodies and other recognition materials, such as their tailorable recognition properties, high selectivity, long life cycles, ease of preparation and low cost.[3] MIPs also exhibit higher stabilities against high temperatures, harsh chemical environments, and extreme pH values. The recognition structures of MIPs can be synthesized as required.[4] These advantages benefit MIPs application in chromatographic separation,[5] solid-phase extraction[6] and biomimetic sensor.[7] MIP-based sensors have been developed, including fluorescent sensors, optical sensors, colorimetric and radiometric binding assays, electrochemical sensors, and mass balances sensors.[8] The major challenges in developing MIP-based sensors include three following respects, poor and moderate affinities and selectivities, limited polymer formats, and integrating MIP with a signaling platform.[9] The imprinting process generates different types of binding sites, and only a small part has highly affinity and selectivity for the template. MIPs have poor selectivities at high analyte concentrations, because of the dominance by the more numerous low-affinity sites, and have low binding capacities at low analyte concentrations, because of the template leaching. To improve MIPs affinities and selectivities, the functional monomers selection and the effective template removal are crucial.[10] In addition, there have been some methods reported about integrating MIPs with signaling platforms, including the electropolymerization of MIPs on conducting surfaces, and the physical adsorption of MIPs on nonconducting surfaces.[11]

Photoluminescent semiconductor quantum dots (QDs) have received much attention over the past few decades. QDs advantages over conventional organic fluorescent dyes include high photoluminescence yields, size-dependent emission wavelengths and high photochemical stabilities. Bruchez *et al.* reported the first biological analysis using QDs, demonstrating the use of QDs as biological probes within living organisms,[12] QDs have since been applied as fluorescent labels for the detection of small molecules, biomolecules and ions.[13] QD-based sensors have also received much attention.[14] Meng *et al.* developed a simple, fast and sensitive biosensor consisting of enzymes, QDs and acetylcholine for detecting organophosphorus pesticides in real samples.[15] Ji *et al.* reported a novel biosensor for detecting paraoxon, by coupling organophosphorus hydrolase to CdSe/ZnS QDs.[16] This was achieved

Key Laboratory of Food Nutrition and Safety, Ministry of Education, Tianjin Key Laboratory of Food Nutrition and Safety, Tianjin University of Science and Technology, Tianjin 300457, China. E-mail: s.wang@tust.edu.cn; Fax: +86 22 60601332; Tel: +86 22 60601430

† Electronic supplementary information (ESI) available: Fig. S1: UV-vis spectra of the extracts from Soxhlet extraction of MIOM (a) and NIOM (b), and UV-vis spectra of CDHB (c), Fig. S2: FT-IR spectra of CDHB, Fig. S3: ^{1}H NMR (A) and ^{13}C NMR spectra (B) of CDHB, Fig. S4: negative ion mass spectra of CDHB, Fig. S5: fluorescence emission spectra of NIOM (a), MIOM before (c) and after (b) template extraction, Fig. S6: fluorescence emission spectra of MIOM (b), NIOM (a), MIOM with addition of 1.56 μmol L^{-1} CDHB (d) and NIOM with addition of 1.56 μmol L^{-1} CDHB (c) in acetonitrile (A), methanol (B) and ethanol (C), separately. See DOI: 10.1039/c3ra45172k

through the electrostatic interaction of negatively charged QDs surfaces with positively charged protein side chain and terminal groups, and the detection limit was about 10^{-8} mol L^{-1}. Incorporating fluorescent QDs as a signaling platform, and selective MIPs as a recognition material, yield optical sensors for target analyte recognition. The MIP would bind the analyte, and the QDs fluorescence intensity would change according to the concentration of the bound analyte. Analyte concentrations can then be converted into optical signals and detected directly by spectrofluorometry.[17] Zhang *et al.* reported a CdSe QD-based MIP-coated composite, for the selective recognition of cytochrome c.[18] Ye *et al.* used a single-bath strategy to synthesize CdTe@SiO_2@MIP for recognizing 4-chlorophenol.[19]

In the current study, the mycotoxin zearalenone (ZON) was used as a target analyte, to illustrate the usefulness of the proposed optical sensor. ZON, also known as F-2 toxin, is mainly produced by Fusarium fungi, and contaminates cereal crops such as corn, barley, sorghum, wheat and oats.[20] ZON causes reproductive problems, infertility in farm animals, and estrogenic effects and possible carcinogenicity in humans.[21] Many countries have regulated acceptable ZON limits in cereals. Austria has established a maximum wheat ZON limit of 60 μg kg^{-1},[22] and the European Union maximum ZON limits for unprocessed maize and unprocessed cereals are 350 and 100 μg kg^{-1} respectively.[20] Various analytical methods have been developed to assay ZON in complex samples including high-performance liquid chromatography (HPLC), fluorophore-linked immunosorbent assay (FLISA), and ultra high pressure liquid chromatography tandem mass spectrometry (UPLC-MS/MS).[5,20,23]

Herein, a molecularly imprinted optosensing material (MIOM) is prepared, using a ZON analog as a template. MIOM is based on ionic liquid (IL)-stabilized CdSe/ZnS (QDs), and is first used for the detection of ZON. The characterization of MIOM was described and discussed in detail.

Experimental

Materials

1,1′-Carbonyldiimidazole, 2,4-dihydroxybenzoic acid, cyclododecanol, 1,8-diazabicyclo[5.4.0]undec-7-ene (DBU), and dimethyl formamide (DMF) were obtained from Aladdin (Shanghai, P.R. China). CdSe/ZnS QDs with a fluorescence emission wavelength of 562 nm were purchased from Jiayuan (Wuhan, P.R. China). The 1-vinyl-3-octylimidazolium hexafluorophosphate IL was purchased from the Chinese Academy of Sciences (Lanzhou, P.R. China). MIOM was prepared using the functional monomer methacrylic acid (MAA; 99%, Tianjin Chemical Reagent Research Institute, Tianjin, P.R. China), cross-linker ethylene glycol dimethacrylate (EGDMA; 98%, Sigma-Aldrich, St Louis, MO, USA) and initiator 2,2-azobisisobutyronitrile (AIBN; 99%, Tianjin Kermel Chemical Reagents Co., Ltd., Tianjin, P.R. China). DMF and MAA were distilled under reduced pressure before use. EGDMA was extracted with 10% NaOH, dried over anhydrous $MgSO_4$, and distilled under reduced pressure. AIBN was recrystallized from ethanol, and stored at 4 °C. ZON, ochratoxin A (OTA) and deoxynivalenol (DON) were obtained from Fermentek (Australia).

Corn, rice and wheat flours were purchased from a supermarket (Tianjin, P.R. China) and ZON-free samples were detected by high-performance liquid chromatography-mass spectrometry (HPLC-MS).

Instruments and measurements

^1H and ^{13}C NMR spectra were recorded on a NMR spectrometer (Bruker BioSpin, Switzerland). Fluorescence measurements were recorded on a Lumina spectrofluorometer (Thermo, USA) equipped with a 1 × 1 cm quartz cell. Ultraviolet-visible (UV-vis) absorption spectra was recorded from 200 to 800 nm, on an Evolution 300 spectrophotometer (Thermo, USA). Fourier-transform infrared (FT-IR) spectra was recorded from 4000 to 400 cm^{-1} using a Tensor 27 FT-IR spectrophotometer (Bruker, Germany). Scanning electron microscopy (SEM; SU1510; Hitachi, Japan) was used to observe the size, shape and surface morphology of MIOM.

Synthesis of cyclododecyl 2,4-dihydroxybenzoate (CDHB)

CDHB was synthesized using a modified reported method.[24] Specifically, 1,1′-carbonyldiimidazole (10 mmol) was mixed with 2,4-dihydroxybenzoic acid (10 mmol) in anhydrous DMF (20 mL). The mixture was stirred at 40 °C in a water bath for 3 h under a N_2 atmosphere. Cyclododecanol (10 mmol) and DBU (10 mmol) were added, and the mixture was stirred for 24 h under N_2. 20 mL of CH_2Cl_2 and 20 mL of water were added to the solution. The organic phase was separated and washed with 10% (v/v) HCl (3 × 30 mL), and saturated NaCl (2 × 30 mL), then dried over anhydrous Na_2SO_4. CDHB was purified through a silica gel column, with a petroleum ether–ethyl acetate (6 : 1) eluent. The removal of solvent at 50 °C, yielded CDHB as a white solid powder.

Preparation of MIOM

CdSe/ZnS QDs (0.05 mmol) and IL (3.0 mmol) were dissolved in chloroform (5.5 mL). The template CDHB (1.0 mmol) and MAA (4.0 mmol) were added, and the solution was stirred for 30 min at room temperature. EGDMA (5.0 mmol) and AIBN (20 mg) were added, and the mixture was purged with N_2 for 5 min to remove any oxygen. The mixture was stirred at 55 °C in a water bath for 24 h in the dark, to allow polymerization. The template was extracted by accelerated solvent extraction (ASE), under the conditions shown in Table 1. Polymers were transferred to a flask for Soxhlet extraction with 4 : 1 (v/v) methanol–acetonitrile until CDHB had been completely removed. Polymers were dried under vacuum at 60 °C for 10 h. Non-imprinted optosensing material (NIOM) was prepared similarly, but in the absence of CDHB.

Fluorescence measurements

The fluorescence detection of MIOM and NIOM was carried out under the same conditions. The excitation and emission slit widths were both 5 nm. The excitation wavelength was 280 nm,

Table 1 ASE conditions for CDHB

Extraction solvent	MeOH–ACN (4/1) (v/v)
Pressure (psi)	1500
Temperature (°C)	60
Heat-up time (min)	10
Static time (min)	10
Flush volume (%)	60
Purge time (s)	60
Number of cycles	3
Cell volume (mL)	66
Number of extractions	2

and emission was recorded at 500–600 nm. The photomultiplier tube voltage was 350 V.

Rebinding, selectivity and competitive adsorption experiments

To evaluate the binding capability of MIOM, 1 mg of MIOM or NIOM was dispersed in 3 mL of certain concentrations of CDHB or ZON. CDHB concentration was 0 to 31.2 μmol L^{-1} in the adsorption equilibrium experiment. ZON concentration was 1.562 μmol L^{-1} in the adsorption kinetic experiment, 0.936 μmol L^{-1} in selective and competitive adsorption experiments. Selectivity and competitive adsorption experiments were carried out using ZON, OTA and DON. OTA and DON are also as mycotoxins in cereals. The mixture was mechanically agitated for a certain time before measurement. The adsorption times were 0 to 8 h in the adsorption kinetic experiment, 7.5 h in the adsorption equilibrium experiment, selective and competitive adsorption experiments.

Analysis of real samples

ZON is often present in the cereal crops including corn, barley, sorghum, wheat and oats. Corn, rice and wheat flours were chosen as samples. Acetonitrile (16 mL) with aqueous NaCl (4 mL, 40 g L^{-1}) were added to corn flours (5 g). The mixture was stirred under vortex conditions for 5 min, ultrasonically extracted for 15 min and then filtered. The filtrate was rotary evaporated to near dryness at 60 °C. The residue was dissolved in acetonitrile for analysis. The recovery study was done by adding ZON to corn flours, at ZON concentrations 50, 100 and 500 ng g^{-1}. The flour–ZON mixture was left to stand for 12 h before extraction. Rice and wheat flours were treated similarly.

Results and discussion

Synthesis of CDHB and MIOM

ZON is expensive and highly toxic, so CDHB was instead used as the template to prepare MIOM. CDHB is similar to ZON in terms of structure, shape, size, functional groups, and hydrophobicity. CDHB has two phenolic hydroxyl groups at the same positions as those in ZON, so it is also able to hydrogen bond with the carboxyl groups of MAA. Hydrophobic CdSe/ZnS QDs modified by trioctylphosphine oxide (TOPO) was used, because CDHB is hydrophobic. Taking into account the negatively charged QDs, the surface of CdSe/ZnS QDs was modified by electrostatic interaction with positively charged IL. IL provided C=C bonds for the QDs to connect with the MIP, and also improved the fluorescence stability of CdSe/ZnS QDs. MAA interacted with IL through the C=C bonds, and the MAA carboxyl group hydrogen bonded with the phenolic hydroxyl groups of CDHB, thus 'pushing' the template into the polymer. Removing the template yielded cavities with shape and functionality complementarity to CDHB, and thus yielded the MIOM.

To demonstrate CDHB was completely removed, we detected UV-vis adsorption of CDHB, and the extracts from Soxhlet extraction. Fig. S1† shows that there were no UV adsorption peaks at 259 and 298 nm in the UV-vis spectra of the extracts, which are the characteristic peaks of the template. The UV-vis spectra of the extracts of MIOM and NIOM were comparable, indicated that the template had been completely removed.

Characterization of CDHB and MIOM

CDHB was characterized by yield, melting point, UV absorptions, IR absorptions, NMR spectra and mass spectra. Specifically: CDHB (2.2 g, 69%), m.p. 57–59 °C, λ_{abs}^{max} (MeOH)/nm 259 (ε/dm^3 mol^{-1} cm^{-1} 17 411), 298 (6724). FT-IR spectra (Fig. S2†), ν_{max}/cm^{-1} 3383 (O–H), 2945 (saturated C–H), 1652 (aromatic C=C), 1519 (aromatic C=C), 1473 (aromatic C=C), 1278 (C–O), 844 and 785 (aromatic C–H). ^{1}H and ^{13}C NMR spectra of CDHB (Fig. S3†) δ_H (400 MHz; DMSO; CDHB) 1.35 (18H, bs, 8–16), 1.57 (2H, bs, 17), 1.76 (2H, bs, 7), 5.17 (1H, m, 6), 6.28 (1H, d, $J = 2.4$ Hz, 2), 6.35 (1H, dd, $J = 2.4$ Hz; 8.8 Hz, 4), 7.62 (1H, d, $J = 8.8$ Hz, 5), 10.44 (1H, s, 1), 10.82 (1H, s, 3). δ_C (DMSO) 20.85 (10), 23.14 (18), 23.36 (11), 23.93 (12), 24.10 (13), 29.09 (14), 39.36 (15), 39.56 (16), 39.77 (17), 39.98 (9), 40.19 (19), 72.73 (8), 102.89 (3), 104.59 (6), 108.71 (1), 131.89 (5), 163.42 (4), 164.70 (2), 169.48 (7) ppm. ESI-MS (Fig. S4†) m/z 319.22 ($[M - H]^-$, 100%). Calculate for $C_{19}H_{28}O_4$: 320.20. The characterization data were in agreement with that reported by Urraca.[24]

SEM images of MIOM and NIOM are shown in Fig. 1, in which MIOM particles appeared spherical and of homogeneous size. NIOM particles' diameters were not as uniform as those of MIOM, and agglomeration to some extent appeared. The possible reason is the MAA dimerization and aggregation. In the MIOM polymerization process, MAA created binding sites including template sites and background sites. While in the NIOM polymerization process, the absence of the template resulted in monomers arranging out of order, and formed background sites rather than template sites. MAA dimerization and aggregation could reduce the number of background sites effectively, but the remaining background sites in NIOM were more than those in MIOM, which made particles agglomerate through MAA forming hydrogen bonded dimers.[10]

The FT-IR spectra of MIOM and NIOM are compared in Fig. 2. Each exhibited the major bands in similar locations, because of their similar compositions. Characteristic peaks were observed at 2993 and 2947 cm^{-1} (saturated C–H), 1731 cm^{-1} (C=O), 1473 cm^{-1} (aromatic C=C), 1398 cm^{-1} (C–O), and 1161 cm^{-1} (C–N). The similarity of these spectra

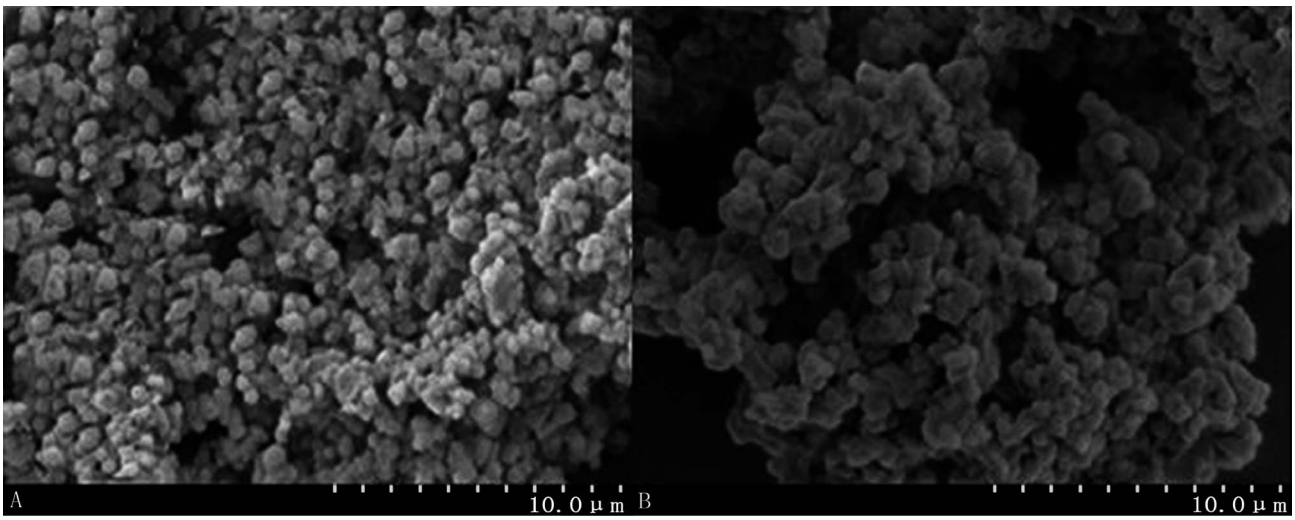

Fig. 1 SEM image of MIOM (A) and NIOM (B).

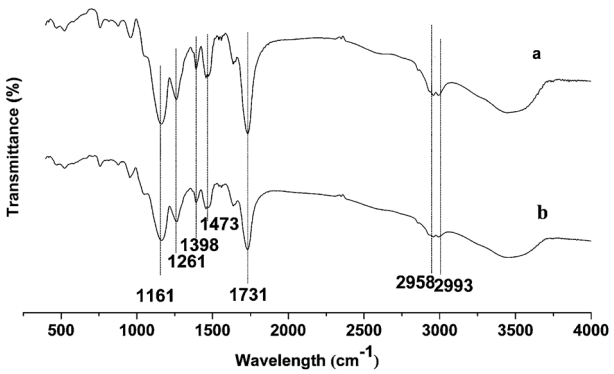

Fig. 2 FT-IR spectra of NIOM (a) and MIOM (b).

suggested that the presence of the template during polymerization and extraction didn't affect the polymer's composition, as predictable from the nature of the non-covalent imprinting process.[25]

Adsorption of MIOM

Fig. S5† shows that before CDHB was extracted, the fluorescence intensity of MIOM was about 64.1% of that of NIOM. After removing CDHB, the fluorescence intensity of MIOM increased, nearly reaching that of NIOM. The fluorescence intensity of MIOM was quenched upon the addition and rebinding of CDHB.

To compare the effects of different solvents on adsorption, MIOM was dispersed in methanol, ethanol and acetonitrile solutions of CDHB. Fig. S6† shows that after adsorption, the degree of MIOM fluorescence quenching in the three solvents is similar. However, the NIOM fluorescence intensity exhibit the smallest decrease in acetonitrile, and the difference in fluorescence intensity between MIOM and NIOM in acetonitrile was obvious. Thus acetonitrile was more suitable for adsorption and was used in the following experiments.

Adsorption equilibrium experiments tend to require more analyte than the adsorption equilibrium experiment and selective experiments. ZON is expensive and highly toxic, so CDHB was used in the adsorption equilibrium experiment. ZON is a trace mycotoxin in food, so low ZON concentration was used to evaluate the rate of mass transfer and the selectivity of MIOM and NIOM toward ZON. The fluorescence intensity of MIOM decreased with increasing CDHB concentration. Fluorescence quenching was mainly caused by hydrogen bonding between MIOM specific binding sites and CDHB. The fluorescence quenching of MIOM and NIOM was quantified by the Stern–Volmer equation:$F_0/F = 1 + K_{SV}[Q]$, where F_0 and F are the fluorescence intensities of the polymers in the absence and presence of quencher, respectively. K_{SV} is the Stern–Volmer constant, and [Q] is the quencher concentration. The ratio of $K_{SV,MIP}$ to $K_{SV,NIP}$ is defined as the imprinting factor (IF), and was used to evaluate the polymer selectivity. ZON was used for adsorption by MIOM and NIOM, to determine their optimal adsorption times. Fig. 3A shows that the optimal adsorption times of MIOM and NIOM were both 7.5 h.

Adsorption equilibrium experiments were carried out to investigate the maximum CDHB adsorption capability of MIOM. Fig. 3B shows that the fluorescence intensity of MIOM gradually decreased with increasing CDHB concentration. There was no further change in the fluorescence intensity of MIOM, when the CDHB concentration reached 15.62 μmol L^{-1}. In contrast, the fluorescence intensity of NIOM exhibited no significant changes, indicating that the affinity of MIOM was much higher than that of NIOM.

The mechanism of fluorescence quenching upon MIOM bonding with ZON was then investigated. MIOM and ZON were dispersed in acetonitrile, respectively, and both were then scanned. Fig. 4 shows that the UV absorption of ZON was close to the MIOM band gap. Thus, charge in the MIOM conduction bands could be transferred to the lowest unoccupied molecular orbital of ZON. Similar charge-transfer mechanisms have been reported by Tu *et al.*[26] Charge transfer from MIOM to ZON was

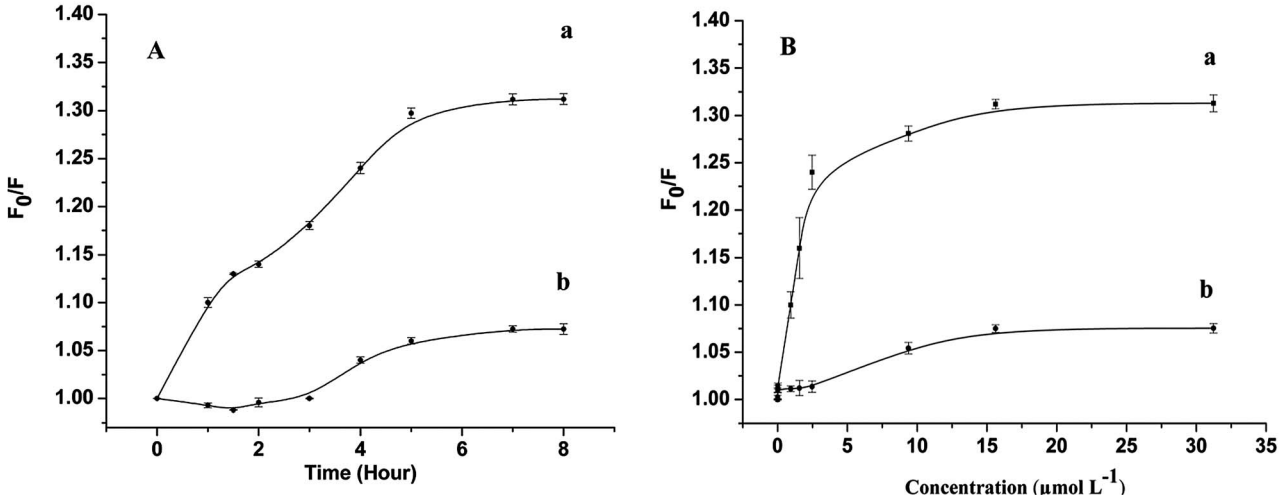

Fig. 3 (A) Kinetic uptake of ZON onto MIOM (a) and NIOM (b). (B) Adsorption equilibrium of MIOM (a) and NIOM (b) rebinding CDHB.

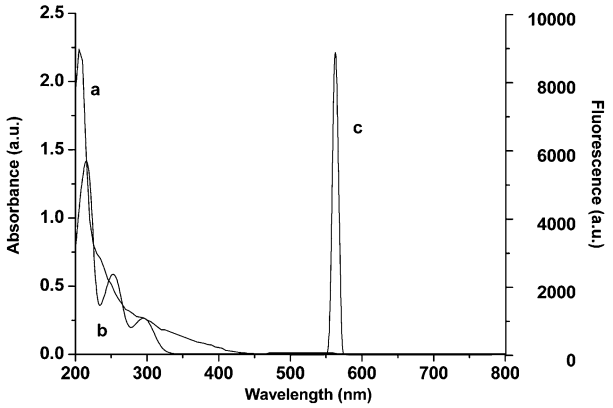

Fig. 4 UV-vis spectra of MIOM dispersed in acetonitrile (a) and ZON standard solution (b), fluorescence emission spectra of QDs (c).

the proposed mechanism of fluorescence quenching. Energy transfer was excluded, because of the absence of spectral overlap between ZON absorption and MIOM emission (562 nm).

Selectivity of MIOM

The mycotoxins ZON, DON, and OTA were used to determinate the selectivity of MIOM towards ZON. ZON, DON and OTA were each separately adsorbed by MIOM. Fig. 5A shows that only ZON resulted in strong fluorescence quenching of MIOM, all three mycotoxins had little effect on the fluorescence of NIOM. Thus, MIOM had a higher adsorption and selectivity for ZON. Fig. 6 shows a comparison of all three tested mycotoxin. While both DON and OTA posses hydroxyl functionality, it differs from that of ZON in terms of location and type. The shape and size of DON and OTA also differ to those of ZON. These factors resulted in

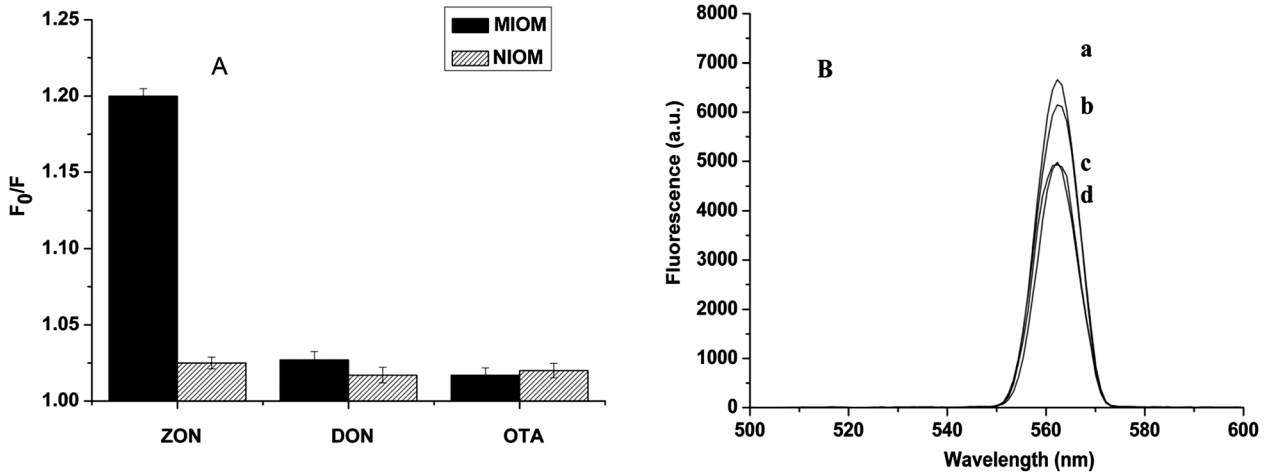

Fig. 5 (A) Selective adsorption of ZON, DON and OTA by MIOM and NIOM. (B) Test for the interference of different mycotoxins on the fluorescence intensity of MIOM (a), MIOM + interfering mixed mycotoxins (b), MIOM + ZON (c), MIOM + ZON + interfering mixed mycotoxins (d). (Interfering mixed mycotoxins: OTA and DON).

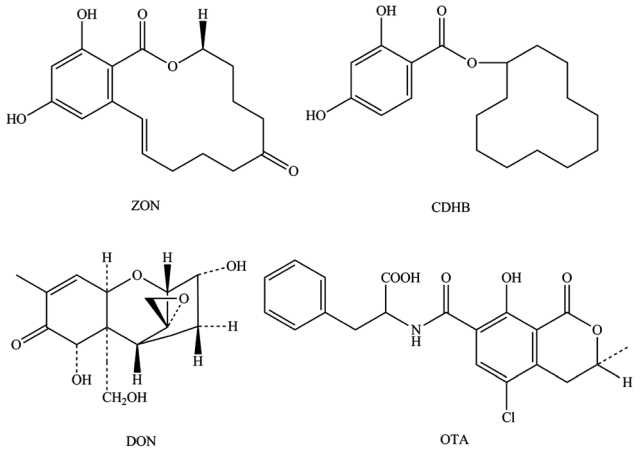

Fig. 6 Structure of CDHB, ZON, DON and OTA.

poor complementarity of DON and OTA with the MIOM binding sites. Thus, the selectivity of MIOM towards DON and OTA was lower than that of ZON.

Competitive adsorption

Analysis of the fluorescence of the MIOM in the presence of mixed mycotoxin solutions was carried out to examine the adsorption ability of MIOM in complex systems. Fig. 5B shows that there was no obvious fluorescence quenching of MIOM, upon adsorbing a mixture of OTA and DON. The fluorescence quenching of MIOM was much larger when adsorbing a mixture of all three mycotoxins or ZON alone. That suggested that any interference of DON and OTA was insignificant. In summary, MIOM can be used as a selective and sensitive recognition material in complex systems. This is because its imprinted binding cavities bind ZON very efficiently.

Detection range and limit

The detection limit and linear range of the MIOM were investigated to evaluate its analytical performance. Fig. 7A shows that the fluorescence intensity of MIOM gradually decreases with increasing ZON concentration. The trend in the MIOM fluorescence quenching obeyed the Stern–Volmer equation, and MIOM exhibited a larger K_{SV} value than NIOM. The IF of MIOM was 42.17 which indicated its high adsorption ability towards ZON. MIOM had a linear range of 0.003–3.12 μmol L^{-1}, with a correlation of 0.9927 for ZON. The detection limit determined as the ZON concentration that quenched three times the standard deviation of a blank signal, divided by the gradient of the standard curve, and was found to be 0.002 μmol L^{-1}. The precision for three replicate detections of a 1.562 μmol L^{-1} ZON solution was 2.2%.

Application to cereal samples

Recovery experiments were carried out to evaluate the MIOM-based method, and the results are shown in Table 2. Recoveries were 94.2–98.7%, 93.1–107.6% and 84.4–106.0% for corn, rice and wheat flour samples, respectively. These values exhibited the potential of MIOM for detecting ZON in real samples.

Table 2 Mean ZON recoveries and relative standard deviations (RSD, %) for cereal samples spiked using various concentration ZON ($n = 3$)

Samples	Spiked amount (ng g^{-1})	Detected amount (ng g^{-1})	Recovery (%)	RSD (%)
Corn flour	50	47.1	94.2	2.6
	100	96.3	96.3	4.7
	500	493.5	98.7	1.2
Rice flour	50	49.2	98.4	7.4
	100	93.1	93.1	4.9
	500	538	107.6	3.0
Wheat flour	50	42.2	84.4	2.8
	100	92.4	92.4	3.9
	500	530	106.0	2.1

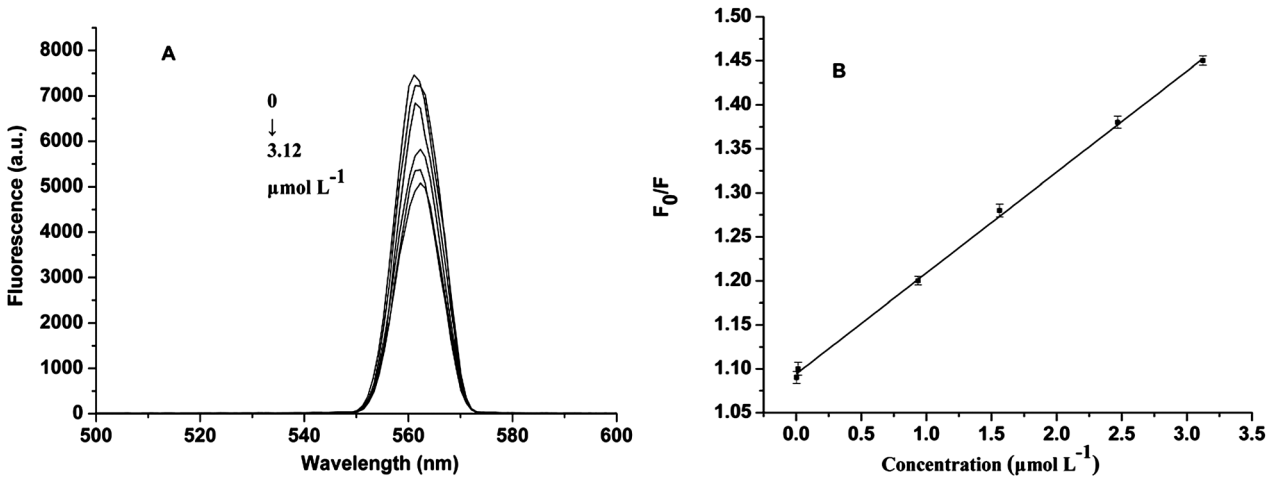

Fig. 7 (A) Fluorescence emission spectra of MIOM with increasing ZON concentration. (B) The ZON concentration calibration curve, error bars = ±standard deviation.

Conclusions

A simple molecularly imprinted optosensing material for detecting ZON in cereal samples was developed. Incorporating the template CDHB into the preparation of MIOM reduced the synthesis cost, and enhances the handling safety. Observing the quenching of fluorescence intensity allowed the determination of ZON concentration as low as 0.002 μmol L^{-1}. MIOM exhibited high selectivity, sensitivity and stability, and could be applied for the detection of ZON in complex matrices. This provides opportunities for higher selectivity analysis.

Acknowledgements

This work was supported by the Ministry of Science and Technology of China (project no. 2012AA101602) and the National Science Foundation for Distinguished Young Scholars of China (project no. 31225021) and General Administration of Quality Supervision, Inspection and Quarantine of the People's Republic of China (Project no. 201210053) and the Program for Changjiang Scholars and Innovative Research Team in University (Project no. IRT1166).

Notes and references

1 G. Wulff and A. Sarchan, *Angew. Chem.*, 1972, **84**, 364; G. Wulff and A. Sarchan, *Tetrahedron Lett.*, 1973, 1329.

2 G. Vlatakis, L. I. Andersson, R. Muller and K. Mosbach, *Nature*, 1993, **361**, 645–647.

3 W. Zhang, X. W. He, Y. Chen, W. Y. Li and Y. K. Zhang, *Biosens. Bioelectron.*, 2012, **31**, 84–89.

4 C. C. Hong, C. C. Lin, C. L. Hong and P. H. Chang, *Biomed. Microdevices*, 2012, **14**, 425–441.

5 J. L. Urraca, M. D. Marazuela and M. C. Moreno-Bondi, *Anal. Bioanal. Chem.*, 2006, **385**, 1155–1161.

6 X. L. Wang, X. G. Qiao, Y. Ma, T. Zhao and Z. X. Xu, *J. Agric. Food Chem.*, 2013, **61**, 3821–3827; X. L. Song, J. H. Li, S. F. Xu, R. J. Ying, J. P. Ma, C. Y. Liao, D. Y. Liu, J. B. Yu and L. X. Chen, *Talanta*, 2012, **99**, 75–82.

7 N. Kirsch, J. P. Hart, D. J. Bird, R. W. Luxton and D. V. McCalley, *Analyst*, 2001, **126**, 1936–1941; T. A. Sergeyeva, S. A. Piletsky, A. A. Brovko, E. A. Slinchenko, L. M. Sergeeva and A. V. El'skaya, *Anal. Chim. Acta*, 1999, **392**, 105–111; S. Kroger, A. P. F. Turmer, K. Mosbach and K. Haupt, *Anal. Chem.*, 1999, **71**, 3698–3702; T. Kobayashi, Y. Murawaki, P. S. Reddy, M. Abe and N. Fujii, *Anal. Chim. Acta*, 2001, **435**, 141–149.

8 A. L. Hillberg, K. R. Brain and C. J. Allender, *Adv. Drug Delivery Rev.*, 2005, **57**, 1875–1889; V. B. Kandimalla and H. Ju, *Anal. Bioanal. Chem.*, 2004, **380**, 587–605; L. Ye and K. Haupt, *Anal. Bioanal. Chem.*, 2004, **378**, 1887–1897; O. Ramstrom and R. J. Ansell, *Chirality*, 1998, **10**, 195–209; T. Takeuchi and J. Haginaka, *J. Chromatogr. Sci.*, 1999, **728**, 1–20; S. Vidyasankar and F. H. Arnold, *Curr. Opin. Biotechnol.*, 1995, **6**, 218–224.

9 Y. G. Zhang and K. D. Shimizu, *Molecular Imprinting and Sensor Development in Chemosensors: Principles, Strategies*, ed. B. H. Wang and E. V. Anslyn, John Wiley & Sons, Inc., Hoboken, New Jersey, 2011, pp. 107–120.

10 Y. G. Zhang, D. Song, J. C. Brown and K. D. Shimizu, *Org. Biomol. Chem.*, 2011, **9**, 120–126; Y. G. Zhang, D. Song, K. D. Shimizu and L. M. Lanni, *Macromolecules*, 2010, **43**, 6284–6294.

11 T. L. Panasyuk, V. M. Mirsky, S. A. Piletsky and O. S. Wolfbeis, *Anal. Chem.*, 1999, **71**, 4609–4613; S. A. Piletsky, H. Matuschewski, U. Schedler, A. Wilpert, E. V. Piletska, T. A. Thiele and M. Ulbricht, *Macromolecules*, 2000, **33**, 3092–3098; T. Panasyuk-Delaney, V. M. Mirsky, M. Ulbricht and O. S. Wolfbeis, *Anal. Chim. Acta*, 2001, **435**, 157–162.

12 M. Bruchez, M. Moronne and P. Gin, *Science*, 1998, **281**, 2013–2016; W. C. W. Chan and S. M. Nie, *Science*, 1998, **281**, 2016–2018.

13 Z. B. Chen, F. X. Ma, X. Liu and L. X. Bian, *Chem. Res. Appl.*, 2011, **23**, 1654–1656; H. Q. Chen, L. Wang, Y. Liu, W. L. Wu, A. N. Liang and X. L. Zhang, *Anal. Bioanal. Chem.*, 2006, **385**, 1457–1461; Z. Y. Yan, D. W. Pang, X. F. Shao and Y. Z. Hu, *J. China Pharm. Univ.*, 2005, **36**, 230–233; H. B. Li, Y. Zhang, X. Q. Wang, D. J. Xiong and Y. Q. Bai, *Mater. Lett.*, 2007, **61**, 1474–1477.

14 L. X. Cheng, X. Liu, J. P. Lei and H. X. Ju, *Anal. Chem.*, 2010, **82**, 3359–3364; G. Jie, H. Huang, X. Sun and J. J. Zhu, *Biosens. Bioelectron.*, 2008, **23**, 1896–1899; G. Liu, J. Wang, J. Kim, M. R. Jan and G. E. Collins, *Anal. Chem.*, 2004, **76**, 7126–7130; H. W. Yu, J. Lee, S. Kim, G. H. Nguyen and I. S. Kim, *Anal. Bioanal. Chem.*, 2009, **394**, 2173–2181; J. Wang, G. Liu, H. Wu and Y. Lin, *Small*, 2008, **4**, 82–86.

15 X. W. Meng, J. F. Wei, X. L. Ren, J. Ren and F. Q. Tang, *Biosens. Bioelectron.*, 2013, **47**, 403–407.

16 X. J. Ji, J. Y. Zheng, J. M. Xu, V. K. Rastogi, T. C. Cheng, J. J. DeFrank and R. M. Leblanc, *J. Phys. Chem. B*, 2005, **109**, 3793–3799.

17 C. I. Lin, A. K. Joseph, C. K. Chang and Y. D. Lee, *Biosens. Bioelectron.*, 2004, **20**, 127–131; Y. Y. Zhao, Y. X. Ma, H. Li and L. Y. Wang, *Anal. Chem.*, 2012, **84**, 386–395.

18 W. Zhang, X. W. He, Y. Chen, W. Y. Li and Y. K. Zhang, *Biosens. Bioelectron.*, 2011, **26**, 2553–2558.

19 T. Ye, S. Y. Lu, Q. Q. Hu, X. Jiang, G. F. Wei, J. J. Wang and J. Q. Lu, *Chin. Chem. Lett.*, 2011, **22**, 1253–1256.

20 N. V. Beloglazova, E. S. Speranskaya, S. De Saeger, Z. Hens, S. Abé and I. Y. Goryacheva, *Anal. Bioanal. Chem.*, 2012, **403**, 3013–3024.

21 W. J. Kang, Y. P. Wang, F. J. Yang, D. F. Tan and R. Ji, *Chin. J. Anal. Lab.*, 2007, **26**, 66–68.

22 M. Tian and W. X. Lin, *Beverage & Fast Frozen Food Industry*, 2003, **9**, 27–29.

23 F. Soleimany, S. Jinap, A. Faridah and A. Khatib, *Food Control*, 2012, **25**, 647–653; B. T. Szabolcs, J. Rita, M. Zoltan and D. Andras, *Chromatographia*, 2011, **73**,

S171–S174; V. P. Nancy, S. Eloy, A. Germán, Messina and R. Julio, *Food Chem.*, 2011, **125**, 791–796.
24 J. L. Urraca, M. D. Marazuela, E. R. Merino, G. Orellana and M. C. Moreno-Bondi, *J. Chromatogr., A*, 2006, **1116**, 127–134.
25 H. L. Liu, D. R. Liu, G. Z. Fang, F. F. Liu, C. C. Liu, Y. K. Yang and S. Wang, *Anal. Chim. Acta*, 2013, **762**, 76–82.
26 R. Y. Tu, B. H. Liu, Z. Y. Wang, D. M. Gao, F. Wang, Q. L. Fang and Z. P. Zhang, *Anal. Chem.*, 2008, **80**, 3458–3465.